Ancestral aryl sulfatases in the alkaline phosphatase family allow for greater increases in catalytic efficiency than extant variants

Bernard Eenink[1], Magdalena Heberlein[1,2], Josephin M. Holstein[2], Andreas Lange[1,*], Carina Dilkaute[3], Tomasz S. Kaminski[4], Erich Bornberg-Bauer[1,5], Joachim Jose[3], Florian Hollfelder[2], Bert van Loo[6]

[1]Institute for Evolution and Biodiversity, University of Münster, Germany
[2]Department of Biochemistry, University of Cambridge, United Kingdom
[3]Institute of Pharmaceutical and Medicinal Chemistry, University of Münster, Germany
[4]Department of Molecular Biology, Institute of Biochemistry, Faculty of Biology, University of Warsaw, Warsaw, Poland
[5]Department of Protein Evolution, Max Planck Institute for Developmental Biology, Tübingen, Germany
[6]Department of Applied Sciences, Northumbria University, Newcastle-upon-Tyne, UK
[*]Corresponding Author: andreas.lange@wwu.de

December 10, 2024

Abstract

Characterizing the dynamics and functional shifts during protein evolution is essential, both for understanding protein evolution and for rationalizing efficient strategies for e.g. enzymes with desired and effective functions.

Most proteins organize in families, sets of divergent sequences which share a common ancestor and a have a similar structural fold.

We study Aryl sulfatases (ASs), a subfamily of the large and evolutionary old alkaline phosphatase superfamily. Together with their computationally reconstructed putative common ancestors, we expressed and enzymatically characterized these enzymes using micro-fluidics generated high-throughput libraries.

We compare the evolvability and robustness of ancestors and four extant ASs which all exhibit catalytic promiscuity towards a range of substrate classes.

Sixteen libraries with distinct mutational loads were expressed in individual cells inside microdroplets.

We find that higher mutational loads yielded a longer tail of active variants but fewer total improved variants.

The effects of mutational load varied quantitatively between enzymes, meaning in some enzymes a higher, in others a lower mutational load was beneficial, highlighting the importance of testing various mutagenesis regimes.

Although ancestors did not display the highest proportion of active variants, they did exhibit the greatest activity increases.

We conclude that in ASs the ancestors are not necessarily more promiscuous but the fitness landscape around them is more shallow and thus more amenable to evolutionary optimization.

Introduction

A fundamental aspect of understanding the intricacies of protein evolution and their structural and functional connections involves categorizing proteins into families [1]. Essentially, protein families are believed to have originated from a shared ancestor through gene duplication, followed by sequence and functional divergence [2, 3], with structural conservation generally being more pronounced [4, 5]. Conversely, to some extent, this apparent conservation arises from structural limitations, which constrain the extent at which sequence modifications can occur before a protein loses its functionality.

Today, it is widely accepted that many enzymes are catalytically promiscuous [6, 7]. Promiscuity contributes to the evolution of new enzymatic functions by offering the organism an initially moderate activity towards non-standard substrates, thereby reducing the distance to the point where this activity provides a selective advantage [7, 8, 9]. Promiscuous enzymes hold promise as a starting point for evolving new enzymes with different activities, potentially starting even before gene duplication [7]. This allows for the rapid design of biocatalysts of novel reactions, such as those needed for green chemistry and breaking down xenobiotics [10].

With directed evolution, protein functions can be enhanced by iterative mutation and selection in the lab, mirroring natural evolution [11, 12]. Directed evolution is utilized to enhance various protein traits such as catalytic efficiency [13], stability [14], enantioselectivity [15] and tolerance to alternative medium conditions [16], broadening the enzyme repertoire for novel or improved reactions. For a successful directed evolution campaign, efficient screening methods and optimal starting sequences are crucial. If the local fitness landscape is in a local maximum this does not allow for gradual improvement towards the desired function. Therefore, increasing the library size itself will not yield the desired outcome [17]. Consequently, understanding the shape of the local fitness landscape is as important as knowing the initial kinetic parameters when selecting a candidate sequence [10, 18]. However, although essential for a successful directed evolution campaign, elucidating the shape of the local fitness landscape is less straightforward than measuring kinetic parameters.

Aryl sulfatases

Aryl sulfatases (AS) are part of the alkaline phosphatase (AP) superfamily. These enzymes catalyze various de-esterification reactions. ASs catalyize the de-esterification of sulfate monoesters, while other members of the family catalyze the de-esterification of phosphate mono- and diesters and phosphonate monoesters [19]. In addition to main reactions, many APs show catalytic promiscuity towards other substrate classes [20]. For this reason the enzymes of the AP superfamily are suitable as a model system for investigating the characteristics and evolvability of ancestral enzymes.

Members of the AP superfamily catalyze the turnover of various substrates with distinct chemistry and different catalytic atoms, by possessing active sites with large, polar surfaces. This lets them facilitate the catalysis of a range of substrates [21]. Promiscuous catalytic activity towards other substrate classes can reach high levels, sometimes on par with the catalytic efficiency of

specific enzymes towards multiple substrate classes [22].

Active multimeric APs have been successfully displayed on the cell surface of *E. coli* by fusing the enzyme to an N-terminal secretion signal and C-terminal autodisplay construct through a linker[23, 20]. This facilitates multimeric AP model systems to be easily screened and efficiently recovered using ultra-high throughput library sorting methods [20].

The AS clade of APs contain a conserved cysteine or serine in the active site that undergoes a post translational modification. In eukaryotic ASs, this modified residue is always a cysteine which is modified into a formylglycine or sometimes a n-serine-semialdehyde [24]. In prokaryotes this is a cysteine or serine that is modified into a formylglycine [25, 26]

Model substrates for ASs are widely available, and can be used to detect sulfate, phosphate and phosphonate esterase activity using a variety of detection methods that makes it suitable as a model system for the screening of high-throughput libraries. 4-nitrophenyl sulfate and 4-nitrophenyl phosphonate can be used for chromophoric assays, fluorescein disulphate and fluorescein diphosphonate can be used for fluorescence assays, and x-sulfate (5-Bromo-4-chloro-3-indoxyl sulfate, Figure 2: **3a**) can be used for agar plate assays [20].

Ancestral sequence reconstruction

Ancestral sequence reconstruction (ASR) is a method used to deduce ancestral sequences at divergent nodes in a phylogenetic tree [27, 28]. Enzymes inferred through ancestral reconstruction exhibit several noteworthy properties such as high thermostability [29, 30, 31] and catalytic promiscuity [30, 32]. Furthermore, these stable ancestral enzymes often show catalytic properties similar to those of mesophilic enzymes, retaining much higher activity at lower temperatures [33]. The debate over whether increased thermostability in inferred ancestral sequences stems from true properties of ancient protein or reconstruction biases persists [34, 35, 36]. However, both possibilities render ancestral proteins as attractive starting points for directed evolution. Less-specific, promiscuous enzymes are easier to adapt towards new functions. Increased thermostability provides a buffer, as function-enhancing mutations, which are often detrimental to the proteins thermostability, will not result in a protein that is too unstable to function. Exploring reconstructed ancestral sequences thus expands the pool of templates for protein engineering beyond natural limits. The propensity of ASR towards thermostable proteins has resulted in a plethora of functional and highly thermostable proteins with unique properties [37]. Increases in thermostability by 20-30 ℃ can be achieved [37]. Furthermore, ancestral proteins have shown promise as scaffolds for computational protein design [38]. Combining ASR with directed evolution opens up new avenues for catalyzing novel reactions. By 're-evolving' an ancestral protein one can both re-navigate the mutational process leading to the present, as well as exploring alternative evolutionary paths by applying different selection pressures in the lab [37].

An excellent example of how ASR helped to understand the evolution of enzymes is the study by Voordeckers et al. [39]. Characterizing a series of glucosidase enzymes, primarily active towards maltose with some activity towards iso-maltose, revealed an inability to optimize both

functions simultaneously. Likewise, comparing malate and lactate dehydrogenases (MDH and LDH), a single mutation in the catalytic site switched enzyme specificity from MDH to LDH. Thus, even minor molecular changes can drastically alter enzymatic function [40]. In another study, enzymes from the CYP1s family were reconstructed [41]. Younger ancestors exhibited increased activity towards environmental carcinogens, while older ancestors displayed increased thermostability. Harris et al. [41] discovered that the oldest ancestor showed a remarkable 35℃ increase in thermostability. Furthermore the common ancestor of a family I.3 bacterial lipolytic enzymes was found to be highly stable, maintaining optimal activity at 70 ℃ and a pH of 10 [42]. ASR has been used both to obtain insight into the evolutionary history of PETases of *Ideonella sakiensis* species as well as obtain highly stable variants with improved catalytic activity towards its PET substrates [43]. Similarly, ASR was used to unravel the evolution of stereoselectivity in flavin-dependent monooxygenases [44]. Besides shedding light on the evolutionary trajectory of enzyme families, these findings prompt inquiries into the sequence landscape surrounding these ancestral nodes. Recently, the mutational landscape around an ancestral fungal laccase was investigated by a combination of directed evolution and structure-guided evolution. Eventually, a variant that oxidized 1,3-cyclopentanedione at a rate 1.6 times that of the ancestral enzyme was found [45]. Their properties make ancestral enzymes of interest for laboratory evolution. As ancestral sequences can be readily expressed in the lab, investigating the sequence space around ancestral, as well as extant enzymes holds promise for uncovering untapped catalytic potential.

Micro-droplet sorting

To screen large amounts of enzyme variants, high-throughput screening methods are required. Water-in-oil emulsion-based micro-droplet sorting enables the screening of large libraries of enzymes and other proteins. The reaction volume is reduced to picoliters, increasing throughput and minimizing reagent usage [46, 47, 48]. By ensuring single occupancy each microdroplet functions as a mini-bioreactor, hosting one cell, or even one plasmid, that produces a single enzyme variant, catalyzing substrate turnover, thus maintaining genotype-phenotype linkage. Droplet sorting has been widely used to screen various classes of enzymes with ultra-high throughput, with both *in vivo* and *in vitro* expression systems [49, 50]. The most straightforward way to mix enzymes and substrate is cell lysis, after which the expression vector can be recovered and sequenced or re-transformed into the host organism [48, 46]. This works well for expression vectors with high copy numbers but when only low copy number vectors are implemented into the screen additional steps need to be taken to recover all sorted diversity [13]. Working with low copy number vectors can be streamlined by cell growth after droplet encapsulation or avoiding lysis by expressing the enzyme in the periplasm or on the surface of the cell [50].

Recent research confirms the viability of using absorption and fluorescence measurements for screening enzymatic activity after cell growth in microdroplet [51, 52]. Recent studies demonstrate the feasibility of conducting droplet sorting experiments with cells that have multiplicated within microdroplets, enhancing sensitivity and post-sorting cell or plasmid recovery, while retaining genotype-phenotype linkage [51, 52]. In these methods, microdroplets containing

growth medium are initially inoculated with individual cells. Subsequently, these individual cells are incubated and multiply, yielding a monoclonal cell population within each microdroplet.

Cell surface display relocates the enzyme from inside the cell to the surface, where it can interact with substrate in the medium, omitting a lysis step and allowing for direct recovery by plating sorted cells on agar plates. In this study we use the *E. coli* autodisplay system (Figure 1) [53, 23], which presents enzymes on the outer membrane. This enables screening and sorting of enzyme libraries with intact, viable cells in microdroplets. Previously, this technique improved the catalytic efficiency of SpAS1 by up to 6.2-fold towards 4-nitrophenyl sulfate and up to 30-fold towards fluorescein disulfate in a single round of directed evolution [13]. The autodisplay system has also demonstrated the ability to express properly folded, active dimeric enzymes [54, 55], including ASs [13].

Aims

In the study presented here our overarching goal is to enable experimental analysis of ancestral and modern properties side-by-side in a parallel experiment using one methodology. This way we can directly compare the properties of ancestral and modern enzymes of the AS-clade of the AP-superfamily, and establish a framework that can be used for characterizing other enzyme families in a similar fashion. To this end we combine FADS[46], the *E. coli* autodisplay system [23, 53], and ASR on aryl sulfatases from the the alkaline phosphatase superfamily [13], particularly the aryl sulfatase (AS) and phosphonate monoester hydrolase (PMH) clades.

We aim to (i) systematically investigate the evolvability (here defined as proportion of variants with improved catalytic efficiency over the wild-type, i.e. beneficial mutations) and robustness (here defined as the proportion of variants that retain wild-type like or better catalytic efficiency, i.e. neutral mutations) of ancestral proteins, (ii) to correlate catalytic efficiency increases observed using high-throughput methods with those seen in cytosolically expressed, purified proteins, and (iii) to investigate the differences and similarities in the local fitness landscapes of various extant and ancestral ASs.

Sulfatase activity was monitored using the FADS with fluorescein disulphate (FDS) as a fluorescent model substrate (Figure 2: **1a**), in microtiter plates using both FDS and 4-nitrophenol sulfate (4NPS) (Figure 2: **2a**) as substrates and on agar plates using x-sulfate (5-Bromo-4-chloro-3-indoxyl sulfate, Figure 2: **3a**) as substrate.

Ancestral AS sequences were previously inferred down to the last common ancestor of the AS and PMH clades [56]. Detailed phylogenetic analysis was performed on extant AS clade members [22]. In this study we describe a parallel directed evolution campaign on four extant and four ancestral AS members for improved catalytic efficiency towards FDS. Autodisplay in *E. coli*, combined with microfluidic FADS, is used to screen and sort living *E. coli* cells presenting unique enzyme variants, with a focus on the shape of the activity distributions of enzyme variants (local fitness landscapes) obtained from FADS sorting (Figure 3).

Materials and Methods

Cloning procedure for cytosole expression

For the cytosolic expression and purification of enzymes, DNA sequences were cloned into the pASKiba5+ vector (Figure 4). Ancestral sequences (Anc496, Anc497, Anc498, Anc499) were cloned using the restriction sites PstI+XhoI, while extant sequences (SpAS2, SaAS, AkAS, RpAS) were cloned using the XhoI+KpnI restriction sites. Subsequently, chemically competent *E. coli* TOP10 cells (INOUE method) were transformed with the assembled plasmid.

Reagents

4-NPS substrate was from Thermo-Fisher. FDS substrate was synthesized as previously described [57]. x-sulfate substrate was from Goldbio.

Cloning procedure for autodisplay

For the expression of individual variants using autodisplay, DNA sequences were cloned into pBAD-AT-shift vector [58] (Figure 4) using the XhoI+KpnI restriction sites. Subsequently, chemically competent (INOUE method) *E. coli* E. cloni 10G cells were transformed with the assembled plasmids.

Library generation methods

Libraries were created using error-prone PCR. In both reactions a mutagenic nucleotide analog, 2'-deoxy-P-nucleoside-5'-triphosphate (dPTP) or 8-oxo-2'-deoxyguanosine-5'-triphosphate (8-oxo-dGTP), respectively, was supplemented into a standard Taq DNA polymerase reaction (GoTaq, Promega). These nucleotide analogs can form pairbonds with multiple nucleotides and can be erroneously incorperated during PCR, when these nucleotide analogs get duplicated again, a different nucleotide may be incorperated in their place. Subsequently a recovery PCR, using the same protocol but not incorperating synthetic nucleotides, was performed on the obtained PCR fragments to remove the incorporated nucleotide analogs. Sequences were then cloned into pBAD-AT-shift using the XhoI+KpnI restriction sites (Figure 4).

Expression of autodisplay constructs

Either glycerol stocks or single colonies on agar plate were used to inoculate 3-10 mL LB medium (100 µg/mL ampicillin) and incubated overnight at 37℃. Overnight cultures were used to inoculate fresh LB medium and incubated at 37℃ until an OD_{600} of +- 0.5. After reaching OD_{600} cells were transferred to expression temperature and incubated for another hour. Cells were then induced by addition of 0.02% L-arabinose and expressed overnight. After overnight expression cells were harvested by centifugation (5 min, 4000*g), resuspended in 1/3 volume SID buffer (pH 7.2, 7.6 or 8.0), according to previously determined pH optima [19][56]. Cells were then washed three times by centifugation (5 min, 4000*g) and resuspended in fresh 1x SID buffer.

Whole cell assays with autodisplayed variants

50-100 µl 1x SID buffer was added to 20-70 µL of resuspended cells for a total volume of 120 µL in a 200 µL microtitre plate. The cell density of each of the cells in each well was measured at OD_{600} before the addition of substrate. 80 µL of 2.5x final concentration **1a** (4NP) or **1b** (FDS) in 1x SID buffer was added for 200 µL final volume. The reaction is measured by increase of absorption value at (400 nm) **1a** (4NP) or fluorescence (λ_{ex} = 490 nm, λ_{em} = 515 nm).

Microfluidic droplet screening

Frozen cells were resuspended in autoinduction medium (LB containing ampicillin 100 mg L^{-1}), L-arabinose (0.04% (v/v) and 0.2% (v/v) D-Glucose. Cell concentration was adjusted to 0.3 cell per droplet volume based on the assumption that OD_{600} = 1 to correspond to 5×10^8 *E. coli* cells mL^{-1}. Droplets were produced in a double flow-focusing junction chip (design: https://openwetware.org/wiki/DropBase:droplet_generation_2_inlets, design iv: 40 µL). First, the autoinduction medium was mixed 1:1 with a solution of 40 µM fluorescein disulfate **1a** in SID buffer pH 7.5 just upstream the flow-focusing (FF) droplet generation junction. At the FF junction, fluorinated oil HFE-7500 (3M) containing 1% (v/v) fluorosurfactant-008 (RAN Biotechnologies) was used to break the continuous stream aqueous phase and generate monodisperse 40 pL droplets with an expected cell occupancy of λ = 0.35 (assuming Poisson distribution). Flow rates were following: 40 µL min^{-1} for both aqueous phases and 160 µL min^{-1} for the oil/surfactant phase. The droplet formation was monitored on an inverted microscope (SP981, Brunell Microscopes) equipped with a high-speed camera (Miro ex4, Phantom Research). The droplets were collected in a droplet chamber (as described in Neun et al., 2020 [59]). Generated droplets were incubated for 1 to 3 days at 30° C. During incubation the cells were aerated [51] by flushing with fluorinated oil HFE-7500 (3M) containing 1% (v/v) fluorosurfactant-008 at a rate of 4 µL per minute. After 2-3 days the droplets were sorted using FADS (as previously described in van Loo et al., 2019 [13], the LABVIEW script used is available online (https://github.com/droplet-lab/spinDrop/tree/main/LabVIEW%20FADS). Droplets were reinjected from the droplet chamber onto a microfluidic chip (design: https://openwetware.org/wiki/DropBase:drop using HFE-7500 (3M) containing 1.5% (v/v) fluorosurfactant-008 (RAN Biotechnologies). Droplets were spaced with oil and pushed through a narrow detection channel to allow single droplet measurement. As the droplets were pushed past a 488 nm laser in the sorting Y-junction, the fluorescent activity inside each droplet as measured by recording emission at 497-553 nm to quantify substrate turnover. Droplets would then flow into a waste channel. When fluorescent activity exceeded a threshold (dependent on wild-type enzyme) pulse and function generators were triggered and generated a square pulse at 8 volts, which was amplified 100-fold by a high-voltage amplifier (610E, Trek) and applied on the sorting device via salt-water electrodes (5 M NaCl). This pulse pulled the selected droplets into a collection channel. The threshold was set to 0.1% of total droplets during a calibration and stabilization phase. Droplets sorted during this phase were discarded, once droplet flow was stabilized and threshold established, collection tubes were added to the collection channel and waste channel and droplet collection started. droplets were collected at a high frequency until a total of 1.000.000 droplets were sorted.

The droplets in the possitive collection channel were collected in a solution of 100 µL Lucigen recovery medium, 45 µl HFE-7500 (3M) and 5 µL PFO surfactant. The collection tubing was fhushed with HFE-7500 (3M) to collect all cells. An additional 500 µL of recovery medium was added after collection and the solution was mixed. The liquid phase was plated on LB+amp plates and incubated overnight.

Blue-White screening

Cells recovered from positive droplets after screening were plated on agar plates (LB+amp) and incubated overnight at 37℃ . Subsequently cells were scraped from plate and replated on a fresh LB+amp plate on top of a nitrocellulose filter. After overnight incubation at 37℃ the nitrocellulose filter was transferred to a fresh LB+amp+arabinose plate and incubated overnight at room temperature to induce expression. The next day nitrocellulose filters were transferred to a fresh LB+amp+arabinose+X-Sulfate plate. Colonies capable of turning over the substrate shifted color towards blue. Colonies with sulfatase activity were identified and counted.

Results and discussion

Selection and confirmation of wild-type and ancestral aryl sulfatases

We reconstructed the aryl sulfatase (AS) and phosphonate monoesterase (PMH) clades of the alkaline phosphatase superfamily down to their last common ancestor ASPMH (Figure 5). We expressed several ancestors of this clade and characterized these ancestors in the lab. We decided to focus on the AS clade as ancestral ASs were more amenable to hetererologous expression in *E. coli*, as well as a broader availability of model substrates.

To compare the evolvability of extant and ancestral enzymes we selected four ancestral members (Anc496, Anc497, Anc498 and Anc499, descending from to the presumed common ancestor of ASPMH) and four extant members (SpAS2, SaAS, AkAS and RpAS) of the AS clade of the previously described AP superfamily [13, 20, 60]. These extant enzymes were selected to obtain a balanced representation of the AS clade, and have previously been successfully expressed and purified [56] (Figure 5). Each represent a sub-clade of the AS clade that descends from ASPMH. We reconstructed the ancestors from SpAS1 down to the common ancestor of ASs, We selected the ancestral enzymes to provide a range of the evolutionary history of ASs.

We successfully expressed each enzyme on the surface of *E. coli*. We confirmed expression and activity of the enzymes by observing the successful turnover of 4-NPS by intact *E. coli* cells surface displaying AS and purification of membrane fractions (Figure S1). We confirmed turnover of 4-NPS for all ancestral (Anc496, Anc497, Anc498 and Anc499) and extant (SpAS2, SaAS, RpAS and AkAS) ASs in the surface display assay. Observed enzyme activities were roughly proportional to those observed in cytosolically expressed and purified proteins.

Creation and screening of mutant libraries

In order to investigate the comparative evolvability of ancestral and extant enzymes, we created error-prone mutant libraries of each ancestral and extant variant. We created mutant libraries through error-prone PCR using either 8-oxo dGTP or dPTP as mutagenic nucleotides to create mutant libraries with distinct mutational profiles (see Methods: Library generation methods). We aimed for a library size of 10^5 variants to obtain a good coverage of single mutations. We tested each colony by transforming the ligation mixture and counting colonies (Table 1) and the successful insertion of each of the genes was determined by colony PCR (Figure S2).

After verifying the size and integrity of each library we transformed the remainder of the ligation mix into *E. coli* and divided the cells equally on agar plates.

All mutant libraries except Anc496 8-oxo dGTP reached the target size of 10^5 unique variants. In total, we screened 16 libraries, representing two different mutational conditions: i) dPTP nucleotides (2.3±1.7 mutations) and ii) 8-oxo dGTP nucleotides (3.7±2.6 mutations) and 8 different enzymes, each either inferred ancestral or extant members of AS clade of the AP-superfamily. We verified the occupancy of the droplets by observing a sample of droplets using confocal microscopy (Figure S3). For each library we screened 10^6 occupied droplets (λ = 0.35). As a control and to form a baseline of wildt-type activity we screened 10^4 occupied

droplets of each respective wild-type enzyme in the same session using the same device for each set.

With the help of FADS up to 10^6 variants could be tested for each library, guaranteeing a large coverage of all possible single mutations and full coverage of the targeted 10^5 sized mutant libraries. Usage of the *E.coli* autodisplay system [23, 53] allowed for the direct recovery of recovered intact cells after screening.

All enzymes that had been previously shown to express solubly and active in cytosolic form [13, 56] also expressed well as autodisplay construct. By using FADS with living cells, it became possible to directly recovering the screened cells and plating them on agar instead of recovering the plasmid that then needs to be re-transformed .

While the rates of improvement varied widely (Figure 6), the overall trend being observed showed a larger increase in improvement in sulfatases having a lower initial activity before mutation. A qualitative effect of mutation rate on enzyme evolvability can also be observed between dPTP (lower mutation rate) and 8-oxo dGTP (higher mutation rate). Here, we observed that a higher mutation rate leads to a decreased improvement in some libraries.

The distribution of extant *SaAS* broadly followed the theorized pattern i.e. that an increased mutation rate leads to a lower number of improved variants. However, the tail of the distribution shows variants with higher activity than in the lower mutation rate library (Figure 6). This implies that variants with more than one mutation are leading to a maximum improvement, and that the coverage of variants with multiple mutations is enough to sort these improved variants. While the library size of 10^5 covers each single mutant, the library does not exhaustively cover double mutations. In Anc497 and Anc498 a different trend is found. In the case of Anc497 most improved variants are seen in the dPTP library while for Anc498 most improved variants are seen in the 8-oxo dGTP library (Figure 6). This distribution sheds light on the shape of the local fitness landscape, as different mutational loads lead to a quantitatively different outcome. Remarkably for RpAS, the enzyme with the greatest wild-type catalytic efficiency, only minor improvements were observed in the libraries, with the majority of the pool of variants performing worse than their wild-type, in both the 8-oxo-dGTP and dPTP libraries. In the SpAS2 library we observed a similar trend, with the bulk of the variants at or below wild-type level, with an extremely low tail of improved variants. For AkAS this was true for the dPTP library, although the 8-oxo-dGTP library showed a tail of improved variants.

Evolvability of ancestral enzymes

Ancestral enzymes, with their enhanced thermostability and substrate promiscuity, are suggested as promising candidates for directed evolution [17, 27, 61]. With the growing accessibility of synthetic DNA, experimental exploration of ancestral enzyme properties has become feasible. To enable direct parallel comparison of ancestral and extant proteins, the mutant libraries were concurrently created using identical methods and backbones.

We assessed the evolvability traits of four extant and four ancestral ASs belonging to the AS-PMH branch of the alkaline phosphatase superfamily (Figure 5).

Our aim was to correlate the evolutionary status of the enzyme with its evolvability and robustness. Leveraging FADS, we conducted high-throughput parallel screening of both modern and ancestral enzyme libraries.

The variation in mutation rates highlights the distinct shape of the local fitness landscape for each enzyme. Earlier studies on malate dehydrogenase and lactate dehydrogenase enzymes already showed that, a single crucial mutation can switch substrate specificity and greatly impact enzyme activity [40]. Given that most mutations are either neutral or destabilizing, stabilizing mutations may be necessary to achieve a functional protein with improved or distinct functions. This contrast may explain the disparity between enzyme backbones capable of attaining novel functionality in one step and those needing additional backbone stabilization to achieve novel function [62, 63].

As expected, the observed mutational landscape varied depending on the enzyme and mutational regime. Naturally, augmenting the mutational load would flatten the curve and possibly elongate the tail in the activity distribution. Given that most mutations are either neutral or detrimental, accumulating multiple mutations raises the likelihood of encountering a deleterious mutation that impairs variant function.

In addition to an increase in impaired variants, one would expect an increase of variants in the tail of the sequence if multiple point mutations are needed to achieve a substantial increase in function. These mutations can either serve as compensatory mutations, necessary to counteract stability loss or folding issues, or as additional mutations directly facilitating changes in function. By introducing multiple mutations in a single round, variants requiring compensatory mutations or epistatic interactions become available. However, each mutation may also cause the enzyme to be non-functional. Here a balance between the possibility of jumping evolutionary 'ratchets' and avoiding the accumulation of deleterious mutations appears. These mutations can be either compensatory mutations, which are required to offset thermostability loss or folding issues or additional mutations. Additional mutations are required to directly facilitate changes in function. Often, while enzymes with different functions differ in many residues, only a few mutations are responsible and sufficient for a change in function [40, 64]. When comparing this phenomena, in which a few mutations are able to greatly shift the activity of an enzyme, to our library screening we observed a similar trend especially in the case of SaAS and AkAS (Figure 6). An interesting case is observed in Anc497, where the dPTP library led to a tail of variants with great improvement, up to 5-fold while the 8-oxo-dGTP library led to much less improved variants, with the top variant showing only half the improvement of most active dPTP variants, as well as sporting much less improved variants (Figure 6. These results are consistent with a unique fitness landscape for each variant, such that the optimal number of mutations to achieve an improvement may vary between enzymes. The histograms indicate that ancestral libraries yielded on average fewer improved variants than the extant enzyme SaAS (Figure 6). However, the ancestors yielded more improved variants than RpAS, SpAS2 or AkAS.

Interestingly, in most ancestral enzymes the lower mutational load dPTP library yielded more improved variants, while the higher mutational load 8-oxo dGTP library yielded more improved

variants in extant enzymes. Overall, these results show that ancestral enzymes can show promise as starting points for directed evolution. When it came to extant enzymes, it showed that the enzymes with greatest starting kinetic parameters showed the least overall improvement, with SaAS outperforming these initially more fit enzymes. Notably, libraries with a lower mutation rate showed a greater tail of improved variants in ancestral libraries, whereas higher mutation rates showed a greater tail of improved variants in extant libraries. This characteristic makes ancestral enzymes especially interesting when screening is limited to lower throughputs due to limitations such as substrate or product detection.

In this study, we integrate microdroplet sorting, autodisplay technology, and Ancestral Sequence Reconstruction (ASR) on the alkaline phosphatase superfamily, focusing on the Aryl sulfatase (AS) and phosphonate monoester hydrolase (PMH) clades [13]. Our objectives were (i) to systematically investigate the evolvability and robustness of ancestral proteins, (ii) to establish a correlation between catalytic efficiency enhancements observed through high-throughput methods and those observed in cytosolically expressed, purified proteins, and (iii) to gain insights into the differences and similarities in the local fitness landscapes of various extant and ancestral As variants.

Conclusion

In this work, we demonstrated that cell-surface-displayed enzyme libraries, grown within droplets, are effective for sorting large libraries—each containing over 10^5 variants—in parallel within a practical time-frame.

When comparing the variant activity histograms of the tested Arylsulfatases (ASs), we found that evolvability was maximized under a lower mutational load for ancestral enzymes while the extant enzymes benefited from a higher mutational load. On the other hand, for the ancestral libraries the lower mutational load dPTP library resulted in a longer tail of improved variants (Figure 6), demonstrating a qualitative difference in the ideal mutational load of different enzymes.

Reconstructed ASs showed a propensity towards needing less mutations for improved function. Therefore ancestral enzymes, particularly in the context of ASs, can serve as valuable initial scaffolds for rapidly achieving significant enhancements in enzyme activity.

Additionally, "imperfect reconstruction"—stemming from less than 100% certainty in assigning residues at ambiguous sites [36]—can be refined through high-throughput directed evolution. Comprehensive coverage of single mutations includes all one-amino-acid-off alternative reconstructions, allowing for the selection of variants that enhance functionality.

An initial directed evolution campaign with multiple (both ancestral and extent) enzymes increases the odds of finding success, as the candidate with optimal initial catalytic efficiency may not have traversable, single/double mutation route towards desired function.

Careful choices will always need to be made concerning library conditions. Several library conditions can be screened in parallel, but exhaustively including all permutations will always explode library size above feasible screening times. Accuracy versus throughput is a consideration throughout the experiment.

This leads to a funnel-like progress where high-throughput screening is used to select winners from a large pool, which are then further characterized using lower throughput microtitre plate screening of variants and finally purified protein.

As ASs typically show promiscuity towards other substrate classes the concept of a low initial activity construct with a broad fitness landscape can be extended towards different enzymes with a promiscuous activity towards the desired reaction.

These results also open up several lines of inquiry for future work. A first line of inquiry is a longer directed evolution campaign starting from improved variants of the best performing ancestral and extant enzyme. Another avenue is expanding the screening from sulfate esters (4NPS and FDS) towards substrates for promiscuous activity towards phosphonate esters and phosphate mono- and di-esters. A further path is screening in parallel through a larger array of conditions such as higher mutation rates or differently biased libraries.

References

[1] Catherine L. Worth, Sungsam Gong, and Tom L. Blundell. Structural and functional constraints in the evolution of protein families, 2009.

[2] Susumu Ohno. *Evolution by Gene Duplication*. Springer Berlin Heidelberg, 1970.

[3] Karin Voordeckers, Chris A Brown, Kevin Vanneste, Elisa van der Zande, Arnout Voet, Steven Maere, and Kevin J Verstrepen. Reconstruction of Ancestral Metabolic Enzymes Reveals Molecular Mechanisms Underlying Evolutionary Innovation through Gene Duplication. *PLOS Biology*, 10(12):e1001446, 12 2012.

[4] Alexey G Murzin, Arthur M Lesk, and Cyrus Chothia. Principles determining the structure of β-sheet barrels in proteins II. The observed structures. *Journal of Molecular Biology*, 236(5):1382–1400, 1994.

[5] Alvaro Ingles-Prieto, Beatriz Ibarra-Molero, Asuncion Delgado-Delgado, Raul Perez-Jimenez, Julio M. Fernandez, Eric A. Gaucher, Jose M. Sanchez-Ruiz, and Jose A. Gavira. Conservation of protein structure over four billion years. *Structure*, 21(9):1690–1697, 2013.

[6] Rinkoo Devi Gupta. Recent advances in enzyme promiscuity. *Sustainable Chemical Processes*, 4(1):2, 2016.

[7] Shelley D Copley. Shining a light on enzyme promiscuity. *Current Opinion in Structural Biology*, 47:167–175, 2017.

[8] P J O'Brien and D Herschlag. Functional interrelationships in the alkaline phosphatase superfamily: Phosphodiesterase activity of E-coli alkaline phosphatase. *Biochemistry*, 40:5691–5699, 2001.

[9] Chetanya Pandya, Jeremiah D Farelli, Debra Dunaway-Mariano, and Karen N Allen. Enzyme Promiscuity: Engine of Evolutionary Innovation. *Journal of Biological Chemistry*, 289(44):30229–30236, 10 2014.

[10] Gloria Yang, Dave W Anderson, Florian Baier, Elias Dohmen, Nansook Hong, Paul D Carr, Shina Caroline Lynn Kamerlin, Colin J Jackson, Erich Bornberg-Bauer, and Nobuhiko Tokuriki. Higher-order epistasis shapes the fitness landscape of a xenobiotic-degrading enzyme. *Nature Chemical Biology*, 15(11):1120–1128, 2019.

[11] Frances H Arnold. Design by Directed Evolution Some Directed Evolution Experiments :. *Accounts of Chemical Research*, 31(3):125–131, 1998.

[12] Philip A Romero and Frances H Arnold. Exploring protein fitness landscapes by directed evolution. *Nature Reviews Molecular Cell Biology*, 10(12):866–876, 2009.

[13] Bert van Loo, Magdalena Heberlein, Philip Mair, Anastasia Zinchenko, Jan Schüürmann, Bernard D G Eenink, Josephin M Holstein, Carina Dilkaute, Joachim Jose, Florian

Hollfelder, and Erich Bornberg-Bauer. High-Throughput, Lysis-free Screening for Sulfatase Activity Using Escherichia coli Autodisplay in Microdroplets. *ACS Synthetic Biology*, 11 2019.

[14] Lori Giver, Anne Gershenson, Per-Ola Freskgard, and Frances H Arnold. Directed evolution of a thermostable esterase. *Proceedings of the National Academy of Sciences*, 95(22):12809 LP – 12813, 10 1998.

[15] Bert van Loo, Jeffrey H.Lutje Spelberg, Jaap Kingma, Theo Sonke, Marcel G Wubbolts, and Dick B Janssen. Directed Evolution of Epoxide Hydrolase from A. radiobacter toward Higher Enantioselectivity by Error-Prone PCR and DNA Shuffling. *Chemistry & Biology*, 11(7):981–990, 2004.

[16] Diana M. Mate, David Gonzalez-Perez, Magnus Falk, Roman Kittl, Marcos Pita, Antonio L. De Lacey, Roland Ludwig, Sergey Shleev, and Miguel Alcalde. Blood Tolerant Laccase by Directed Evolution. *Chemistry & Biology*, 20(2):223–231, 2013.

[17] Devin L. Trudeau and Dan S. Tawfik. Protein engineers turned evolutionists—the quest for the optimal starting point. *Current Opinion in Biotechnology*, 60:46–52, 2019.

[18] Jia Zheng, Joshua L Payne, and Andreas Wagner. Cryptic genetic variation accelerates evolution by opening access to diverse adaptive peaks. *Science*, 365(6451):347–353, 2019.

[19] Bert van Loo, Stefanie Jonas, Ann C Babtie, Alhosna Benjdia, Olivier Berteau, M. Hyvonen, and Florian Hollfelder. An efficient, multiply promiscuous hydrolase in the alkaline phosphatase superfamily. *Proceedings of the National Academy of Sciences*, 107(7):2740–2745, 2010.

[20] Bert van Loo, Christopher D. Bayer, Gerhard Fischer, Stefanie Jonas, Eugene Valkov, Mark F. Mohamed, Anastassia Vorobieva, Celine Dutruel, Marko Hyvönen, and Florian Hollfelder. Balancing Specificity and Promiscuity in Enzyme Evolution: Multidimensional Activity Transitions in the Alkaline Phosphatase Superfamily. *Journal of the American Chemical Society*, 141(1):370–387, 2019.

[21] Anna Pabis, Fernanda Duarte, and Shina C L Kamerlin. Promiscuity in the Enzymatic Catalysis of Phosphate and Sulfate Transfer. *Biochemistry*, 55(22):3061–3081, 2016.

[22] Bert van Loo, Markus Schober, Eugene Valkov, Magdalena Heberlein, Erich Bornberg-Bauer, Kurt Faber, Marko Hyvönen, and Florian Hollfelder. Structural and Mechanistic Analysis of the Choline Sulfatase from Sinorhizobium melliloti: A Class I Sulfatase Specific for an Alkyl Sulfate Ester. *Journal of Molecular Biology*, 430(7):1004–1023, 2018.

[23] Joachim Jose. Autodisplay: Efficient bacterial surface display of recombinant proteins. *Applied Microbiology and Biotechnology*, 69(6):607–614, 2006.

[24] Thorsten Selmer, Armin Hallmann, Bernhard Schmidt, Manfred Sumper, and Kurt Von Figura. The evolutionary conservation of a novel protein modification, the conversion

of cysteine to serinesemialdehyde in arylsulfatase from Volvox carteri. *European Journal of Biochemistry*, 238(2), 1996.

[25] Thomas Dierks, Claudia Miech, Jörg Hummerjohann, Bernhard Schmidt, Michael A. Kertesz, and Kurt Von Figura. Posttranslational formation of formylglycine in prokaryotic sulfatases by modification of either cysteine or serine. *Journal of Biological Chemistry*, 273(40), 1998.

[26] Thomas Dierks, M. Rita Lecca, Petra Schlotterhose, Bernhard Schmidt, and Kurt Von Figura. Sequence determinants directing conversion of cysteine to formylglycine in eukaryotic sulfatases. *EMBO Journal*, 18(8), 1999.

[27] Y. Gumulya and E. M. J. Gillam. Exploring the past and the future of protein evolution with ancestral sequence reconstruction: the 'retro approach to protein engineering. *Biochemical Journal*, 474(1):1–19, 2017.

[28] Rainer Merkl and Reinhard Sterner. Ancestral protein reconstruction: Techniques and applications. *Biological Chemistry*, 397(1):1–21, 2016.

[29] M Luisa Romero-Romero, Valeria A Risso, Sergio Martinez-Rodriguez, Beatriz Ibarra-Molero, and Jose M. Sanchez-Ruiz. Engineering ancestral protein hyperstability. *The Biochemical journal*, 18(5):592–6, 2016.

[30] Valeria A. Risso, Jose A. Gavira, Diego F. Mejia-Carmona, Eric A. Gaucher, and Jose M. Sanchez-Ruiz. Hyperstability and substrate promiscuity in laboratory resurrections of precambrian B-lactamases. *Journal of the American Chemical Society*, 135(8):2899–2902, 2013.

[31] Lucas C. Wheeler, Shion A. Lim, Susan Marqusee, and Michael J. Harms. The thermostability and specificity of ancient proteins. *Current Opinion in Structural Biology*, 38:37–43, 2016.

[32] Petra Babkova, Eva Sebestova, Jan Brezovsky, Radka Chaloupkova, and Jiri Damborsky. Ancestral haloalkane dehalogenases show robustness and unique substrate specificity. *ChemBioChem*, 2017.

[33] Ryutaro Furukawa, Wakako Toma, Koji Yamazaki, and Satoshi Akanuma. Ancestral sequence reconstruction produces thermally stable enzymes with mesophilic enzyme-like catalytic properties. *Scientific Reports*, 10(1), 2020.

[34] Devin L. Trudeau, Miriam Kaltenbach, and Dan S. Tawfik. On the Potential Origins of the High Stability of Reconstructed Ancestral Proteins. *Molecular Biology and Evolution*, 33(10):2633–2641, 2016.

[35] Amanda K Garcia, J William Schopf, Shin-ichi Yokobori, Satoshi Akanuma, and Akihiko Yamagishi. Reconstructed ancestral enzymes suggest long-term cooling of Earth's photic zone since the Archean. *Proceedings of the National Academy of Sciences*, 114(18):4619–4624, 5 2017.

[36] Geeta N Eick, Jamie T Bridgham, Douglas P Anderson, Michael J Harms, and Joseph W Thornton. Robustness of reconstructed ancestral protein functions to statistical uncertainty. *Molecular Biology and Evolution*, 34(2):247–261, 2016.

[37] Yosephin Gumulya, Jong-Min Baek, Shun-Jie Wun, Raine E S Thomson, Kurt L Harris, Dominic J B Hunter, James B Y H Behrendorff, Justyna Kulig, Shan Zheng, Xueming Wu, Bin Wu, Jeanette E Stok, James J De Voss, Gerhard Schenk, Ulrik Jurva, Shalini Andersson, Emre M Isin, Mikael Bodén, Luke Guddat, and Elizabeth M J Gillam. Engineering highly functional thermostable proteins using ancestral sequence reconstruction. *Nature Catalysis*, 1(11):878–888, 2018.

[38] Gaspar P. Pinto, Marina Corbella, Andrey O. Demkiv, and Shina Caroline Lynn Kamerlin. Exploiting enzyme evolution for computational protein design, 2022.

[39] Voordeckers Karin and Chris A A N D Vanneste Kevin A N D van der Zande Elisa A N D Voet Arnout A N D Maere Steven A N D Verstrepen Kevin J Brown. Reconstruction of Ancestral Metabolic Enzymes Reveals Molecular Mechanisms Underlying Evolutionary Innovation through Gene Duplication. *PLOS Biology*, 10(12):1–17, 11 2012.

[40] Jeffrey I Boucher, Joseph R Jacobowitz, Brian C Beckett, Scott Classen, and Douglas L Theobald. An atomic-resolution view of neofunctionalization in the evolution of apicomplexan lactate dehydrogenases. *eLife*, 3:e02304, 6 2014.

[41] Kurt L Harris, Raine E S Thomson, Yosephine Gumulya, Gabriel Foley, Saskya E Carrera-Pacheco, Parnayan Syed, Tomasz Janosik, Ann-Sofie Sandinge, Shalini Andersson, Ulrik Jurva, Mikael Bodén, and Elizabeth M J Gillam. Ancestral Sequence Reconstruction of a Cytochrome P450 Family Involved in Chemical Defense Reveals the Functional Evolution of a Promiscuous, Xenobiotic-Metabolizing Enzyme in Vertebrates. *Molecular Biology and Evolution*, 39(6):msac116, 6 2022.

[42] Mohamad Farihan Afnan Mohd Rozi, Raja Noor Zaliha Raja Abd Rahman, Adam Thean Chor Leow, and Mohd Shukuri Mohamad Ali. Ancestral sequence reconstruction of ancient lipase from family I.3 bacterial lipolytic enzymes. *Molecular Phylogenetics and Evolution*, 168, 2022.

[43] Yvonne Joho, Vanessa Vongsouthi, Matthew A. Spence, Jennifer Ton, Chloe Gomez, Li Lynn Tan, Joe A. Kaczmarski, Alessandro T. Caputo, Santana Royan, Colin J. Jackson, and Albert Ardevol. Ancestral Sequence Reconstruction Identifies Structural Changes Underlying the Evolution of Ideonella sakaiensis PETase and Variants with Improved Stability and Activity. *Biochemistry*, 62(2), 2023.

[44] Chang Hwa Chiang, Troy Wymore, Attabey Rodríguez Benítez, Azam Hussain, Janet L. Smith, Charles L. Brooks, and Alison R.H. Narayan. Deciphering the evolution of flavin-dependent monooxygenase stereoselectivity using ancestral sequence reconstruction. *Proceedings of the National Academy of Sciences of the United States of America*, 120(15), 2023.

[45] Bernardo J. Gomez-Fernandez, Valeria A. Risso, Andres Rueda, Jose M. Sanchez-Ruiz, and Miguel Alcalde. Ancestral resurrection and directed evolution of fungal mesozoic laccases. *Applied and Environmental Microbiology*, 86(14), 2020.

[46] Philip Mair, Fabrice Gielen, and Florian Hollfelder. Exploring sequence space in search of functional enzymes using microfluidic droplets. 2017.

[47] Itay Levin and Amir Aharoni. Evolution in microfluidic droplet. *Chemistry and Biology*, 19(8):929–931, 2012.

[48] Fabrice Gielen, Raphaelle Hours, Stephane Emond, Martin Fischlechner, Ursula Schell, and Florian Hollfelder. Ultrahigh-throughput-directed enzyme evolution by absorbance-activated droplet sorting (AADS). *Proceedings of the National Academy of Sciences of the United States of America*, 113(47):E7383–E7389, 2016.

[49] Jianhua Yang, Ran Tu, Huiling Yuan, Qinhong Wang, and Leilei Zhu. Recent advances in droplet microfluidics for enzyme and cell factory engineering, 2021.

[50] Maximilian Gantz, Stefanie Neun, Elliot J. Medcalf, Liisa D. van Vliet, and Florian Hollfelder. Ultrahigh-Throughput Enzyme Engineering and Discovery in In Vitro Compartments, 2023.

[51] Paul Jannis Zurek, Raphaëlle Hours, Ursula Schell, Ahir Pushpanath, and Florian Hollfelder. Growth amplification in ultrahigh-throughput microdroplet screening increases sensitivity of clonal enzyme assays and minimizes phenotypic variation. *Lab Chip*, 21(1):163–173, 2021.

[52] Bernard D.G. Eenink, Tomasz S. Kaminski, Erich Bornberg-Bauer, Joachim Jose, Florian Hollfelder, and Bert van Loo. Vector redesign and in-droplet cell-growth improves enrichment and recovery in live Escherichia coli. *Microbial Biotechnology*, 15(11), 2022.

[53] Joachim Jose, Ruth Maria Maas, and Mark George Teese. Autodisplay of enzymes-Molecular basis and perspectives. *Journal of Biotechnology*, 161(2):92–103, 2012.

[54] Florian Lenz, Paul Zurek, Martina Umlauf, Iasson E.P. Tozakidis, and Joachim Jose. Tailor-made β-glucosidase with increased activity at lower temperature without loss of stability and glucose tolerance. *Green Chemistry*, 22(7), 2020.

[55] Katrin Gesing, Florian Lenz, Sebastian Schreiber, Matthias Kasimir, Hans Ulrich Humpf, and Joachim Jose. Surface Display and Engineering of Laccase CotA for Increased Growth of Pseudomonas putida on Lignin. *ChemCatChem*, 16(4), 2024.

[56] Magdalena Heberlein. *Evolution of substrate specificity in the alkaline phosphatase superfamily*. PhD thesis, 2016.

[57] John Scheigetz, Michael Gilbert, and Robert Zamboni. Synthesis of fluorescein phosphates and sulfates. *Organic Preparations and Procedures International*, 29(5), 1997.

[58] Jan Schüürmann, Paul Quehl, Fabian Lindhorst, Kristina Lang, and Joachim Jose. Autodisplay of glucose-6-phosphate dehydrogenase for redox cofactor regeneration at the cell surface. *Biotechnology and Bioengineering*, 114(8), 2017.

[59] Stefanie Neun, Paul J Zurek, Tomasz S Kaminski, and Florian Hollfelder. Chapter Thirteen - Ultrahigh throughput screening for enzyme function in droplets. In Dan S Tawfik, editor, *Methods in Enzymology*, volume 643, pages 317–343. Academic Press, 2020.

[60] Patrick C.F. Buchholz, Bert Van Loo, Bernard D.G. Eenink, Erich Bornberg-Bauer, and Jürgen Pleiss. Ancestral sequences of a large promiscuous enzyme family correspond to bridges in sequence space in a network representation. *Journal of the Royal Society Interface*, 18(184), 2021.

[61] Miguel Alcalde. When directed evolution met ancestral enzyme resurrection. *Microbial Biotechnology*, 0:0–2, 2016.

[62] Rinkoo D Gupta and Dan S Tawfik. Directed enzyme evolution via small and effective neutral drift libraries. *Nature methods*, 5(11):939–942, 2008.

[63] Devin L. Trudeau, Miriam Kaltenbach, and Dan S. Tawfik. On the Potential Origins of the High Stability of Reconstructed Ancestral Proteins. *Molecular Biology and Evolution*, 33(10):2633–2641, 2016.

[64] Arvind S. Pillai, Georg K.A. Hochberg, and Joseph W. Thornton. Simple mechanisms for the evolution of protein complexity, 2022.

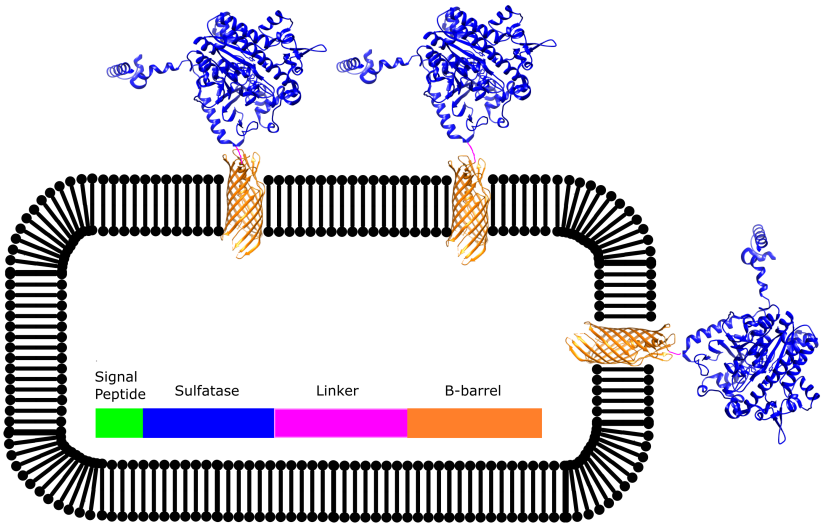

Figure 1: Schematic overview of the sulfatase enzymes displayed on the outer membrane of *E. coli* cells. A signal peptide directs the fused protein towards the periplasmic space where the AIDA β-barrel folds into the outer membrane and displays the passenger enzyme at the surface [52, 53].

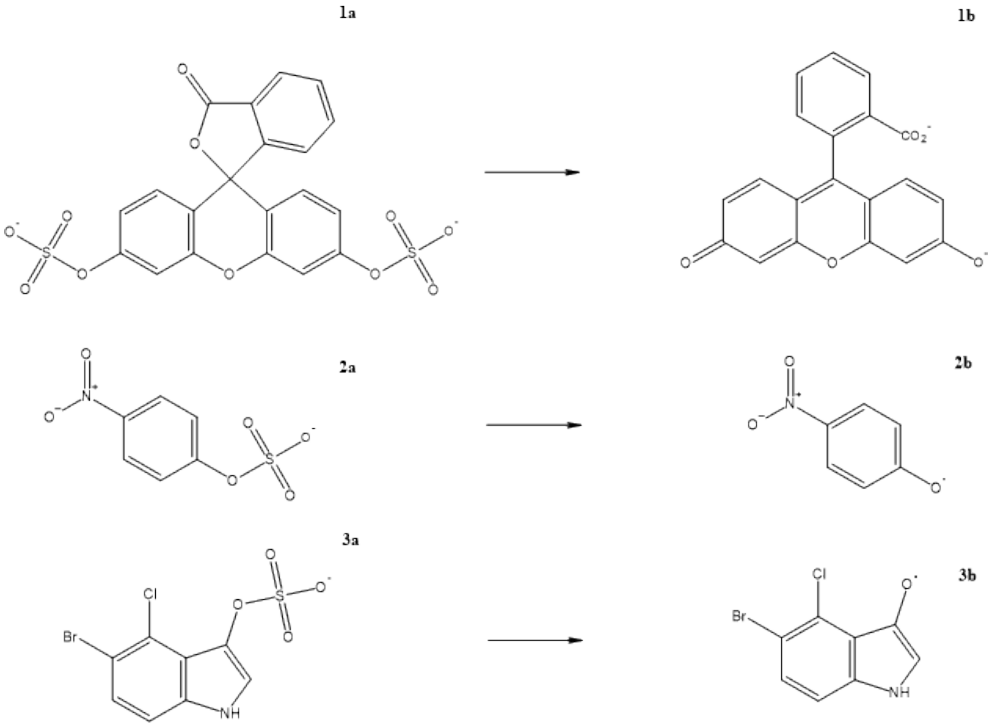

Figure 2: Overview of reactions used to measure enzyme activity. Turnover of Fluorescein disulfate (1a) into Fluorescein (1b) was used for droplet and microtitre plate screening, turnover of 4-nitrophenol sulfate (2a) into 4-nitrophenol, and turnover of X-sulfate (3a) into desulfated X-sulfate (3b).

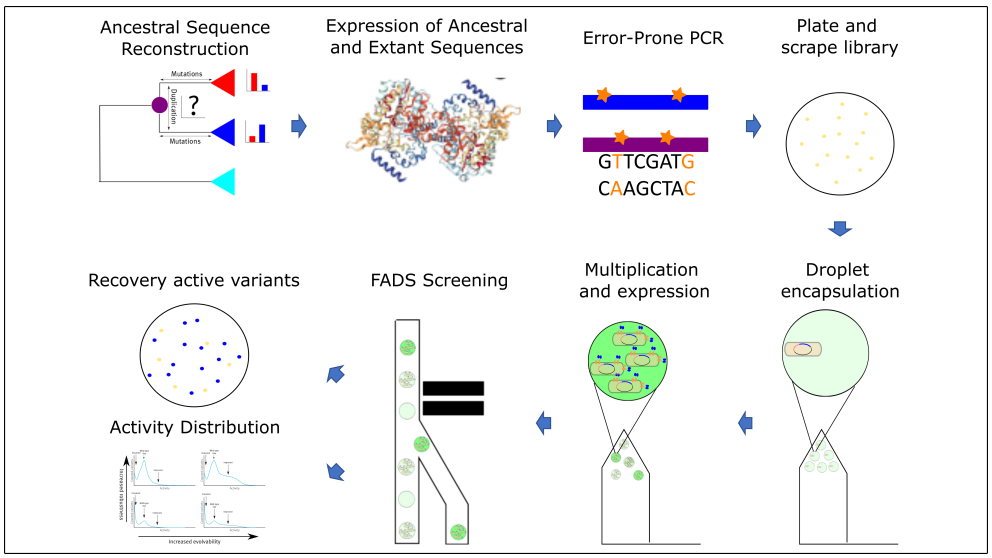

Figure 3: Overview of the protocol used. Ancestral enzymes were reconstructed using ASR, ancestral and extant enzymes were expressed in the lab using the AIDA autodisplay construct, error-prone PCR using synthetic nucleotide analogs was done on a library of each enzyme after which *E. coli* cells were transformed with the libraries. Variants were encapsulated into microdroplets and screened using FADS after which active variants were recovered and the activity distribution of screened variants was measured.

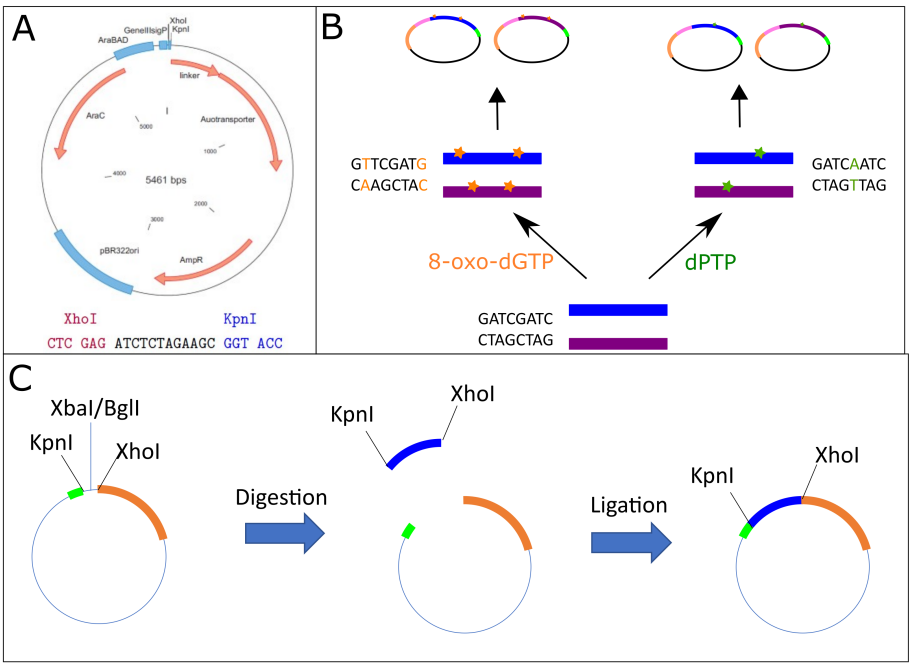

Figure 4: Overview of plasmid engineering used in the study. pBAD-AT-shift (A) was used for all vector engineering. epPCR libraries were generated by spiking the PCR reaction with the synthetic nucleotides 8-oxo-dGTP (yellow) and dPTP (green), which each have a unique substitution profile and a different mutation rate (B). PCR generated libraries were cloned into the pBAD-AT vector [58] using KpnI and XhoI restriction sites, in this vector, the gene of interest (blue) is fused to an n-terminal signal peptide encoding sequence (green) and fused to a c-terminal β-barrel encoding sequence through a linker, as required for the transport of the passenger (e.g. the AS variants) to the cell surface. The vector was treated with XbaI to remove any un-ligated uncut plasmid prior to ligation (C).

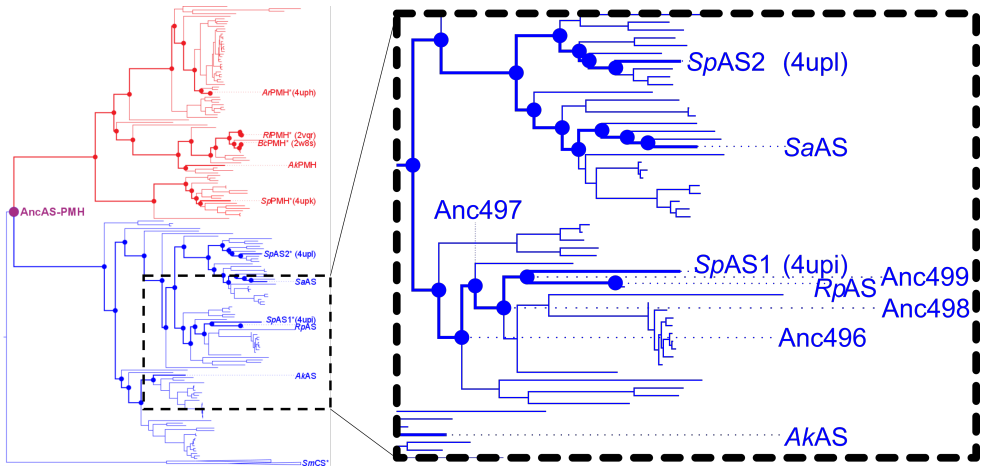

Figure 5: Phylogenetic tree of the AS and PMH clades of the Alkaline superfamily leading back to the common ancestor of AS and PMH. Dots represent inferred ancestral states of the PMH (red) and AS (blue) clade. Wildtype enzymes used in the study are labeled. Inferred ancestral enzymes reconstructed and used in the study are labeled in blue.

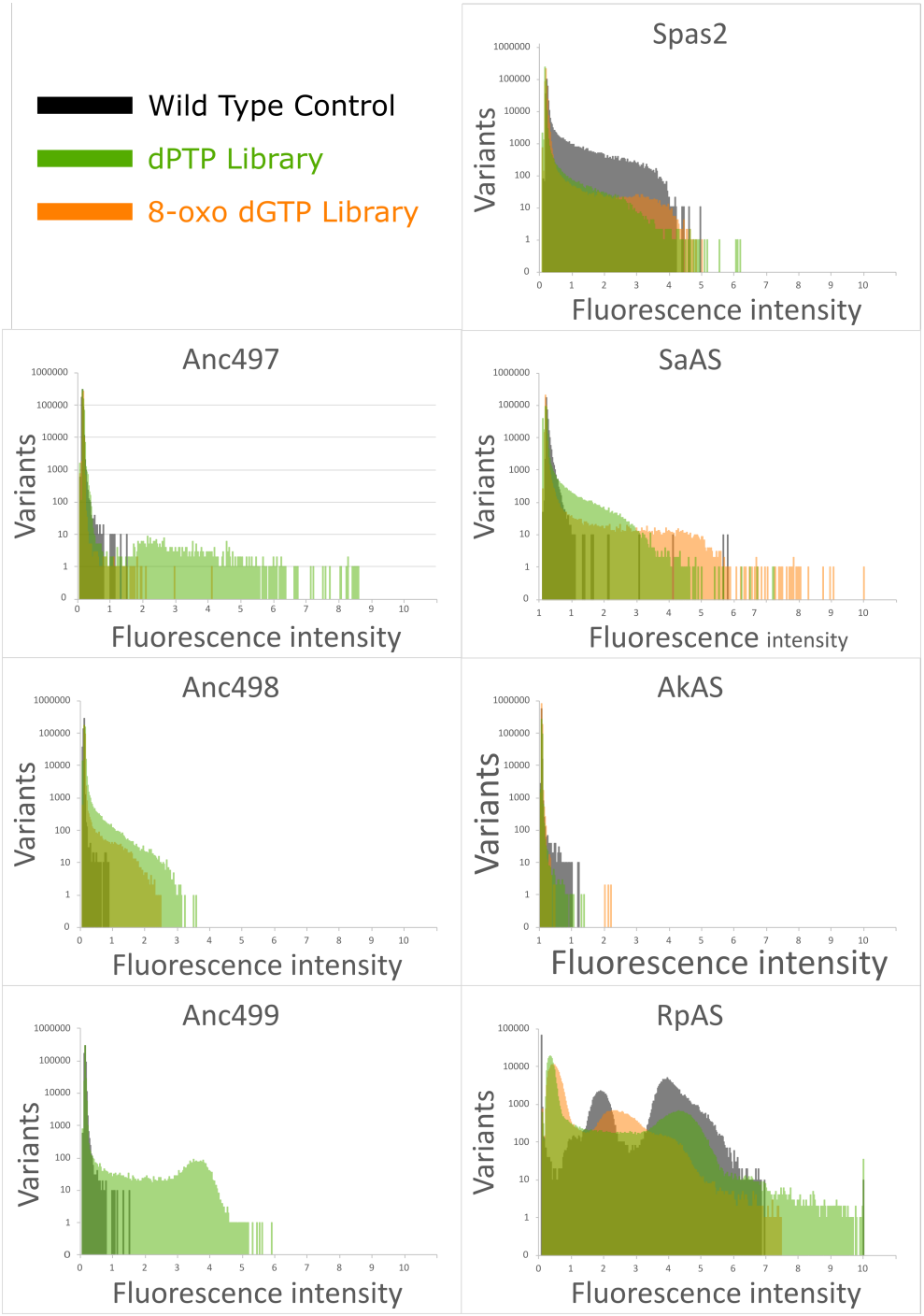

Figure 6: Activity distribution of each ancestral and extant enzyme. 1.000.000 individual droplets were screened using FADS. Libraries shown are dPTP (green) and 8-oxo-dGTP (orange). To measure the baseline activity of each enzyme 100.000 wild-type variants of each variant were screened (black).

Library	estimated size
Anc496 8-oxo dGTP	55.800
Anc496 dPTP	690.000
Anc497 8-oxo dGTP	228.000
Anc497 dPTP	426.000
Anc498 8-oxo dGTP	462.000
Anc498 dPTP	396.000
Anc499 8-oxo dGTP	270.000
Anc499 dPTP	450.000
SpAS2 8-oxo dGTP	270.000
SpAS2 dPTP	1.926.000
SaAS 8-oxo dGTP	750.000
SaAS dPTP	402.000
AkAS 8-oxo dGTP	360.000
AkAS dPTP	1.236.000
RpAS 8-oxo dGTP	822.000
RpAS dPTP	1.218.000

Table 1: Estimated sizes of each generated library, library sizes were determined by extrapolating from dilution plates.

Variant	"Age"	Tm
Anc496	0.70	55.1
Anc497	0.72	57.4
Anc498	0.75	49.6
Anc499	0.78	48.6
Spas1	0.98	46.4
SpAS2	0.98	51.7
SaAS	1.00	49.5
AkAS	0.68	45.6
RpAS	0.90	47.05

Table 2: Thermostability of extant and ancestral wild-types.